PCCP

Accepted Manuscript

ROYAL SOCIETY OF CHEMISTRY

www.rsc.org/pccp

Physical Chemistry Chemical Physics RSCPublishing

COMMUNICATION

Gold Nanocrystal Arrays as a Macroscopic Platform for Molecular Junction Thermoelectrics

Cite this: DOI: 10.1039/x0xx00000x

W. B. Chang[a*], B. Russ[b,c*], V. Ho[c], J.J. Urban[b], and R.A. Segalman[a]

Received 00th January 2012,
Accepted 00th January 2012

DOI: 10.1039/x0xx00000x

www.rsc.org/

Abstract: Efficiencies of bulk thermoelectric systems have been limited because the Seebeck coefficient and electrical conductivity are typically inversely correlated in traditional materials. Decoupling of these properties has been demonstrated in molecular junctions by capitalizing on the unique electronic transport at organic-inorganic interfaces. In this work, the thermoelectric properties of gold nanocrystal arrays with varying thiol-terminated ligands are compared to molecular junction experiments. The experimental results and supporting theory demonstrate that gold nanocrystal arrays are a valuable model system for mapping the applicability of molecular junction design rules to the design of macroscale organic-inorganic hybrid thermoelectric materials.

INTRODUCTION

Thermoelectrics are a promising avenue for waste heat conversion to usable electrical energy. The efficiency of thermoelectrics is related to the thermoelectric figure of merit, ZT, and is described by the following Equation 1:

$$ZT = \frac{S^2\sigma}{\kappa}T \qquad \text{(Eq. 1)}$$

where the Seebeck coefficient, S, and the electrical conductivity, σ, define the power factor, $S^2\sigma$, and, κ is the thermal conductivity. In most materials, the Seebeck coefficient and the electrical conductivity are inversely correlated, limiting the power factor. To achieve greater efficiencies in thermoelectrics, these material properties must be individually controlled and decoupled. Single molecule studies have shown promise in changing the relationship between the Seebeck coefficient, S, and electrical conductance, G, (the single molecule equivalent of the electrical conductivity) with experiments demonstrating simultaneous increases in S and G.[1] While an ideal model system for studying thermoelectrics on a fundamental level, single molecule junctions must be scaled to multi-dimensional architectures to fulfil the promise of being active components in devices and applications.[2] Nanocrystal arrays (NCAs) have already proven to be useful platforms for investigating macroscale molecular junction-induced thermal[3-4] and optoelectronic material properties.[5,6,7] We demonstrate in this work that NCAs are also attractive model systems for studying the scalability of molecular junction thermoelectric design principles.

We selected gold nanoparticles with organic surface ligands for fabricating our macroscale model of molecular junction arrays. Arrays of gold nanoparticles were an ideal material choice, providing a direct multi-dimensional system parallel to gold scanning tunnelling microscope (STM)-break junction tips.[8,9] Advances in ligand exchange strategies on the nanoparticle surface[5] enable an avenue to controllably tailor the molecular junctions throughout a NCA.[10,11] From the single molecule literature, a series of monothiol (alkanethiols) and dithiol (alkanedithiols and oligophenyldithiols) ligands were chosen with varying molecular junction lengths. The thermoelectric properties of single molecule junctions with these ligands have been theoretically and experimentally determined, providing a robust reference for comparison to the NCA studies.[12,13,14] In our study, the thiol binding group was held constant to eliminate variables such as binding geometry and strength of electrode coupling, which can both significantly influence transport.[15]

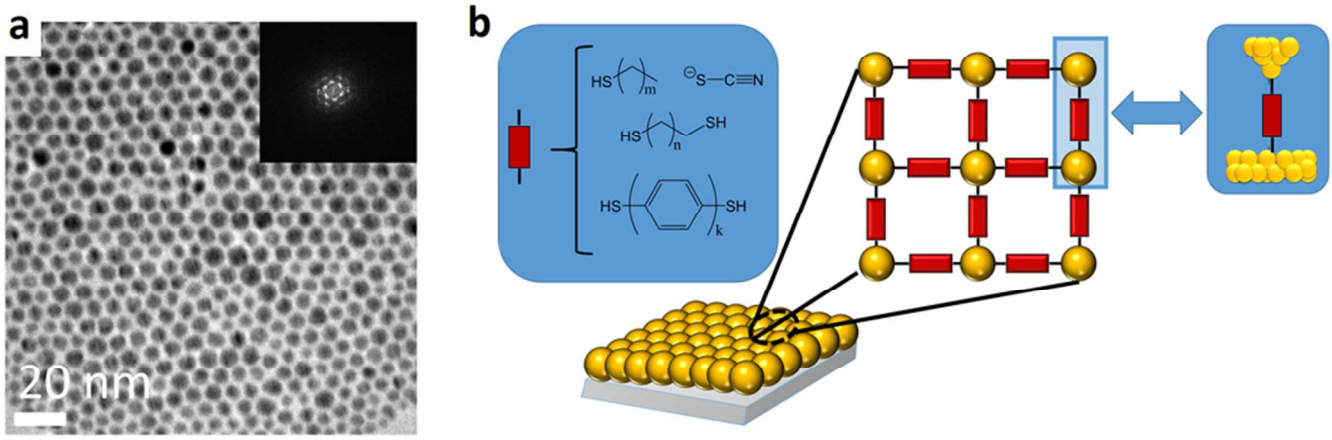

Figure 1: (a) Transmission electron microscopy of drop-casted gold nanocrystal arrays with oleylamine ligands, with a scale bar of 20 nm. Inset: the Fourier transform of this image shows the well-ordered nature of the thin film with oleylamine ligands (R_{mean} = 3 nm, σ_R = 1.5 nm). Exchanged SEM images of the gold NCA films can be found in the SI (S1-S4). (b) Schematic of gold nanocrystal arrays used as a model system for mapping the applicability of molecular junction design rules to the design of macroscale organic-inorganic hybrid thermoelectric materials. Three classes of thiol-terminated ligands were used in these studies for comparison to previously reported single molecule experiments: monothiol terminated ligands [thiocyanate and alkanethiols (m=1,2,3,4)] and two types of dithiol terminated ligand systems [alkanedithiols (n=1,2,3,5,7) and oligophenyldithiols (k=1,2,3)]. A single Au-ligand-Au element is highlighted to emphasize its similarity to the gold STM-break junction tips in single molecule experiments.

METHODS

Gold nanoparticles were synthesized following procedures reported previously.[16] 500 mg of gold (III) chloride hydrate (Sigma Aldrich) and 12.5mL of oleylamine were mixed with 62.5 mL toluene in a 250 mL flask. The solution was kept stirring under nitrogen for six hours at 65°C. The solution changed colours from orange to deep purple over the course of the reaction time. It was then cooled and 50 mL of ethanol were added to the reaction mixture and centrifuged at 6000 rpm for 3 min. The supernatant was removed and the precipitate dispersed in 3 mL heptane. To make samples for thermoelectric characterization, glass substrates were sequentially sonicated in the following series of solvents for 15 minutes each: water with 2% liquid alkaline detergent, water, 1M HCL, water, and ethanol. The substrates were then placed in a 5% filtered mercaptopropyl-trisilane in toluene solution overnight, and then sequentially rinsed in toluene, 50/50% toluene/ethanol, and ethanol. 20 µl of the 10 mg/ml Au NP solution was then drop-casted on the cleaned substrates. Upon drying under a heat lamp, films of approximately 1 µm thickness (1cm^2 in length) were obtained.

The NCAs are closed packed FCC arrays, with individual nanoparticles five to seven nanometers in diameter. A representative TEM of the gold NCA with native oleylamine ligand is shown in Figure 1a. Fourier transform of the image in Figure 1a demonstrates the degree of ordering in these films. Ligand exchange from oleylamine to monothiol terminated ligands (thiocyanate and alkanethiols) and dithiol terminated ligands (alkanedithiols and oligophenyldithiols) of varying lengths was performed in the solid state, with each film placed in a two percent solution of the desired ligand in acetone for two hours, and then washed with acetone.[17] All ligand molecules were obtained from Sigma- Aldrich (chemical structures depicted in Figure 1a). After exchange, the film undergoes changes in porosity with some cracking observed, as shown in SEM images S1-S4. However, the films remain well-connected electrically and thermally after exchange[11], and nanoparticle sizes did not change significantly. Ideally, the gold nanocrystal array is envisioned to represent the schematic in Figure 1b. TEM imaging was conducted on a JEOL JEM-2100 microscope at an operating voltage of 200 kV. Films were prepared by spin-coating a dilute nanoparticle solution from a 1:1 Octane:hexane mixture (1000 rpm, 30s) onto silicon nitride grids (Ted Pella, 50 nm thick). Scanning Electron Microscopy (SEM) imaging was conducted on a Zeiss FESEM-Ultra55 at an operating voltage of 5 kV. Drop cast gold nanoparticle thin films for SEM were prepared on silicon substrates (1cmx1cm).

Using a Nicolet 6700 FTIR-ATR, successful ligand exchange was confirmed by the disappearance of the characteristic IR amine stretch at 3000 cm^{-1} from the oleylamine (SI S5).[18] Thin film absorption spectra were collected using a Cary 50 UV-VIS-NIR spectrometer. Drop-cast gold nanoparticle thin films for the UV-VIS-NIR measurements were prepared on glass substrates (1cmx1cm). The UV-VIS spectra for exchanged gold NCAs with the various dithiol ligands are shown in SI S6. All the UV-VIS spectrums of dithiol exchanged films show a different surface plasmon resonance peak than a film of Au NCA with oleylamine ligands, indicating a different dielectric environment for the gold nanoparticles due to ligand exchange.

Electrical conductivity measurements were made in a four point probe Van der Pauw configuration using Keithley 2400 source meters. Seebeck coefficient measurements were made in a two point probe configuration; a Keithley 2010 was used to sense the thermoelectric voltage under a temperature gradient applied via two Peltier heaters, one at an elevated temperature, and the counterpart held at room temperature. To obtain accurate average Seebeck coefficient readings, one thousand open circuit voltage data points

were collected at each applied temperature difference, an approach which parallels the large sample statistics applied to single molecular junction thermoelectric measurements and done on triplicate films.

RESULTS AND DISCUSSION

Our experiments show that electron tunnelling from gold nanoparticle to nanoparticle follows an exponential decay with inter-particle separation distance, and electrical conductance can be correlated to the length of single molecule junctions in the framework of the electron tunnelling model.[19] In single molecular experiments, electrical conductance is facilitated by transmission through a molecular orbital in the junction. These molecular orbitals are hypothesized to be metal induced gap states (MIGS), and can be visualized in SI S7. In this transport regime, the Landauer transmission function dictates electron transport,[20] and the magnitude of resistance increases exponentially with length, as seen in Equation 2:

$$R = R_A e^{\beta L} \quad \text{(Eq. 2)}$$

where R is the electrical resistance, the inverse of conductance, R_A is the extrapolated resistance at zero length, β is the electronic decay parameter, and L is the ligand or molecular junction length.

The ligand length dependence of electrical conductance in the exchanged gold nanocrystal arrays displays a prominent similarity to trends observed for single molecule junctions.[21] Figure 2 shows how the electrical resistivity changes exponentially with increasing ligand lengths in these NCAs, measured in triplicate (error bars are on the scale of the data points). The yellow diamond is the resistivity of a thermally evaporated 100nm thick gold film, which serves as the control for intrinsic conductivity of gold. The red triangles refer to monothiol ligands binding with a gold adatom (with increasing length: ammonium thiocyanate, ethanethiol, propanethiol, butanethiol and pentanethiol, β = 2.3 Å^{-1}). The blue squares are alkanedithiol ligands (with increasing length: ethanedithiol, propanedithiol, butanedithiol, hexanedithiol, octanedithiol, β = 0.95 Å^{-1}). The black circles represent oligophenyldithiol ligands (benzenedithiol, biphenyldithiol, terphenyldithiol, β = 0.05 Å^{-1}). Ligand lengths were calculated using Spartan'14, and a table is provided in the SI T1. The thiocyanate ligands studied are classified as monothiols, like alkanethiols, due to their preference for mono-dentate thiol binding on gold atoms and inability to form bi-dentate bonds.

Notably, each class of ligand exhibits an exponential increase in the electrical resistivity with increasing ligand length, but the magnitude of the β decay parameter depends strongly on molecular conjugation and whether the ligand is monothiol or dithiol. Alkanedithiol NCAs has a β decay parameter of 0.95 Å^{-1}, which is similar to the value seen for single molecule alkanedithiol junctions, where a β decay parameter of 0.88 Å^{-1} is reported.[22] Oligophenyldithiols in the single molecule literature typically exhibit smaller β decays than alkanedithiols, due to the presence of conjugation along the molecular backbone. This trend is also observed in NCAs with oligophenyldithiols, with a β decay parameter of 0.05 Å^{-1}. In the single molecule literature, oligophenyldithiols have been observed to have a β decay parameter of 0.26 Å^{-1}.[23] The overall trends between classes of organic molecular ligands hold in the nanocrystal arrays. Given the macroscopic nature of the transport in gold nanocrystal arrays, it is reasonable to expect some deviation in absolute β decay values from the single molecule measurements.

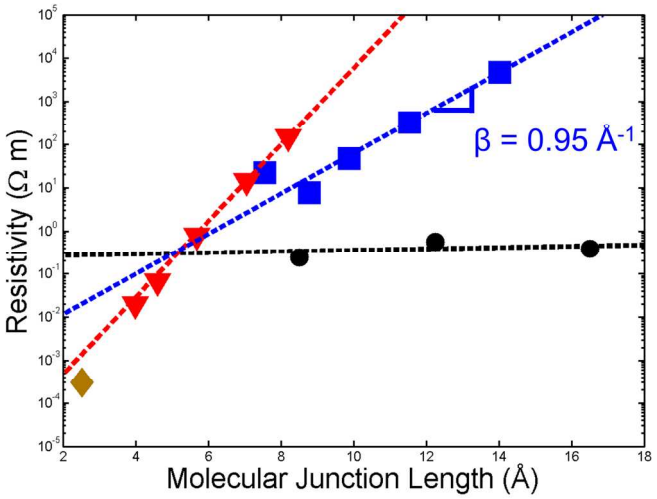

Figure 2: Electrical resistivity of gold nanocrystal arrays as a function of ligand length is shown. β decay parameters for thiocyanate and alkanethiols (red triangles), alkanedithiols (blue squares) and oligophenyldithiols (black circles) are 2.3 Å^{-1}, 0.95 Å^{-1}, 0.05 Å^{-1} respectively. A 100nm gold thin film resistivity is the yellow diamond. Conjugation along the molecular backbone in oligophenyldithiols results in a lower decay parameter than in alkanedithiols. Error bars are on the scale of the data points.

While an increase in the electrical resistance with increasing ligand length was anticipated, it was surprising to observe that the Seebeck coefficient of these gold nanocrystal arrays switches from positive to negative in alkanethiols (Figure 3). A positive Seebeck coefficient indicates p-type (hole) transport, while a negative Seebeck coefficient demonstrates n-type (electron) transport. The colour scheme and naming in Figure 3 corresponds identically to that of Figure 2, with the exception of the absence of octanedithiol, which has a Seebeck coefficient so low that it was indistinguishable from the noise floor. With increasing alkane ligand length, a switch from p-type behaviour to n-type behaviour is observed at approximately 6 Ångstroms in alkanethiol NCAs. Error bars based on measurements of three separate films are on the scale of the data points.

Alkanedithiol NCAs show n-type transport, and a Seebeck coefficient that decreases in magnitude with ligand length. The relationship between the Seebeck coefficient and alkanedithiol length is 0.51 μV/(K Å). In contrast, the Seebeck coefficient of alkanedithiols in single molecule measurements is reported to be positive, indicating p-type transport, and the change in Seebeck coefficient as a function of length has been observed to be -0.74 μV/(K Å), with ethanedithiol exhibiting a Seebeck coefficient of 6.8 μV/K.[24] In both single molecule junctions and NCAs, increasing alkanedithiol length results in a decreased Seebeck coefficient, albeit with different carrier type. Reproducing the switch in sign of the Seebeck coefficient in alkanedithiols NCAs as seen in the alkanethiol NCAs was not experimentally feasible, as the only alkanedithiol shorter than ethanedithiol is methandithiol, an unstable chemical compound.

Oligophenyldithiols (black, Figure 3 inset) show a much larger Seebeck coefficient than alkanedithiols, with Seebeck

coefficients of 40 μV/K. In the single molecule literature, oligophenyldithiols consistently show Seebeck coefficients that increase with molecule length, and have values much higher than alkanedithiols, with typical values of 6.3 μV/K observed for ethanedithiol and 8.7 μV/K for benzenedithiol.[24] However, in the NCA film measurements, there is no discernible trend with oligophenyldithiols length versus Seebeck coefficient, which shows a peak value with biphenyldithiol. The large size and steric stiffness of terphenyldithiols, as compared to alkanedithiols, potentially introduce film defects during ligand exchange, which could explain the absence of a ligand size dependence of the Seebeck coefficient.

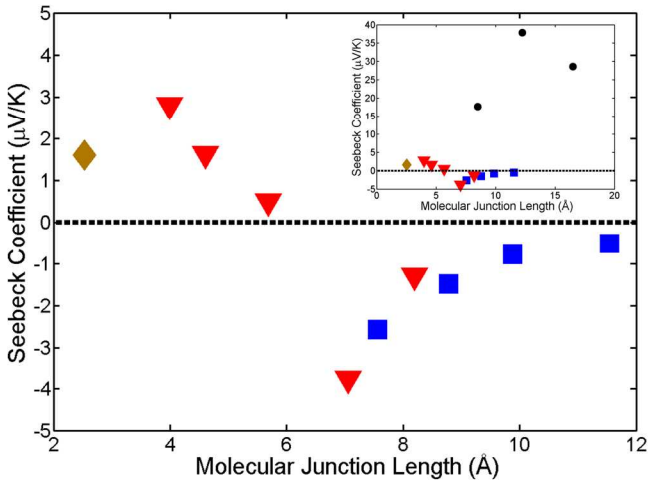

Figure 3: The Seebeck coefficient of gold nanocrystal arrays as a function of ligand length for thiocyanate and alkanethiols (red triangles) and alkanedithiols (blue squares). As molecular junction length increases, a switch from hole transport to electron transport is observed at approximately 6 Ångstroms. The error bars are on the scale of the data point. (Inset) Oligophenyldithiols (black circles) show a much higher Seebeck coefficient than alkanedithiols (blue squares), as predicted from the single molecule literature.

Several physical changes within the nanocrystal arrays are hypothesized to explain the origin of the n-type transport observed in the alkanedithiol system and the p-n type switch in alkanethiol NCAs. Small angle x-ray scattering experiments were performed to see if an order-disorder transition was present, since an ordered film could show different carrier transport than a disordered film.[25] However, as shown in S7, the peak intensity decreases substantially upon ligand exchange, indicating that all films are disordered post-exchange, and thus this explanation cannot hold.

An alternative explanation for the observed transport behaviour involves modulation in the MIGS energy levels. In single molecule junction theory, the Seebeck coefficient is directly related to the slope of the logarithm of the Landauer transmission function at the Fermi energy, with the sign of the slope dictating whether the charge transport is n-type or p-type.[13] The transmission through MIGS decreases in probability as the single molecule length decreases; as a result, the magnitude of the Seebeck coefficient diminishes as well.[26] This correlation between ligand length and the Seebeck coefficient matches what is observe experimentally in gold NCAs with dithiol ligands as well in NCAs with monothiol ligands for the two longest ligand lengths. Changes in the energy level of the MIGS have also been hypothesized and experimentally verified to induce p-type to n-type switches in the Seebeck coefficient in single molecule junctions at a critical ligand length.[27] While we did not observe the switch in Seebeck sign in NCAs with dithiol ligands, possibly limited by the minimum ligand lengths experimentally accessible for exchange, the switching transport behaviour observed with shorter monothiol ligands in gold NCAs may be associated with the MIGS energy level modulation phenomena. Experimental verification of MIGS in gold NCAs with ultraviolet photoelectron spectroscopy is on-going.

To accurately compare the thermoelectric behaviour between single molecule junctions and nanocrystal array films, the theoretical power factor $S^2\sigma$ was calculated using the theory developed by Müller.[28] The power factor of a nanocrystal array was theoretically modelled based on the constituent molecular junction experimental thermoelectric properties. It can be shown that the Seebeck coefficient and electrical conductivity of the NCA is described by Equation 3 & 4:

$$S_{NCA} = S_{Junction} \quad \text{(Eq. 3)}$$

$$\sigma_{NCA} = \frac{N_Y N_Z}{N_X L} M G_{Junction} \quad \text{(Eq. 4)}$$

Where $N_{x,y,z}$ is the number of junctions in a given dimension, L is the nanoparticle diameter, M is the number of molecules bridging a junction, $G_{junction}$ is the electrical conductance of a single molecule junction, and $S_{junction}$ is the Seebeck coefficient of said junction. Given the sample geometry and knowledge of the nanoparticle size from TEM, and an approximation of the number of ligands participating in electron transmission at 1000 molecules (see SI Eqn 1 for the calculation), the theoretical power factor of a nanocrystal array based on molecular junction theory can be determined. This is shown in Figure 4, which directly compares the theoretical power factor of a gold NCA based on experimental single molecule experiments to experimental nanocrystal array power factors. The theoretical power factor predictions are well matched in both trend and value to those observed experimentally for alkanedithiols. In contrast, the predicted power factor of oligophenyldithiols is markedly lower than what is observed experimentally. This disparity is due to the conductivity of oligophenyldithiols being higher in NCAs than predicted from the single molecule literature, which may result from better energy level alignment at the gold nanoparticle/ligand interface than in single molecule junctions. Multiple ligands binding to the same nanoparticle has been predicted to modulate the MIGS level, an effect not seen in molecular junctions consisting of only a single molecule.[28]

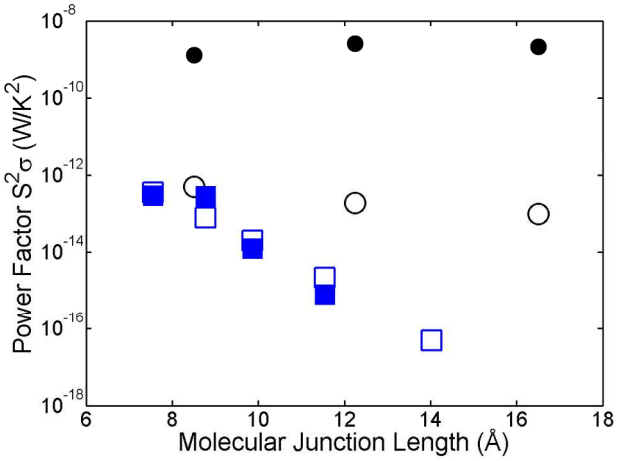

Figure 4: Comparison of the power factor $S^2\sigma$ in gold NCAs with

alkanedithiol ligands (blue, filled squares) and oligophenyldithiols (black, filled circles) compared to theoretical NCAs based on STM/AFM break junction single molecule experiments (alkanedithiols in blue, open squares and oligophenyldithiols in black, open circles. The prediction from theory fits well to alkanedithiol experimental data with the parameters: L = 10 nm, $N_yN_z/N_x = 10^{-7}$ junctions, M = 1000 molecules.

Conclusion

In this work, we demonstrate the potential for using gold nanocrystal arrays to investigate the applicability of single molecule junctions design rules to macroscale thermoelectric materials. When scaling single molecule junctions to fully functionalized nanocrystal arrays, the ligand length dependence of the electrical conductivity draws a direct parallel to the length dependence of single molecule junction electrical conductance ($\beta_{conjugated}<\beta_{non\text{-}conjugated}$). The ligand length dependence of the Seebeck coefficient was in partial agreement with single molecule literature. Like with molecular junctions, increasing alkanedithiol length decreases the Seebeck coefficient in NCAs. However, the presence of alkanethiol ligands in NCAs resulted in an intriguing p-type to n-type switch in electrical transport with increasing ligand length. While the full nature of this transition is not yet well understood, these results suggest that it may be possible to use surface ligand design to selectively modulate the dominant charge carriers involved in electrical transport, a topic of great interest to the materials community at large. Within the theoretical framework discussed in this manuscript, we believe that two promising routes for enhancing the thermoelectric transport in NCAs are: (1) improving the transport efficiency of individual ligands and (2) increasing the number of ligands participating in inter-particle transport. Based on the high performance demonstrated by oligophenyldithiols in our study, continued efforts are underway to investigate the impact of alternative, highly conjugated ligands. Furthermore, control of particle geometry to improve film packing density in NCAs may help increase the quantity of transport-participating ligands and is also the subject of ongoing research. These initial studies on gold NCAs demonstrate the development of a model platform to build on single molecule thermoelectric research and guide the design of organic-inorganic hybrids that decouple traditionally linked material properties.

Acknowledgements

This work was supported by AFOSR MURI FA9550-12-1-0002.

Notes and references

[a] Department of Materials, University of California, Santa Barbara, CA 93117

[b] Lawrence Berkeley National Laboratory, 1 Cyclotron Road, MS 67R4110, Berkeley, CA 94720.

[c] Department of Chemical and Biomolecular Engineering, University of California, Berkeley, CA 94720-1462 D.

* These authors contributed equally.

Electronic Supplementary Information (ESI) available. See DOI: 10.1039/c000000x/

1. K. Baheti, J. A. Malen, P. Doak, P. Reddy, S.-Y. Jang, T. D. Tilley, A. Majumdar, and R. A. Segalman, *Nano Lett.*, 2008, **8**, 715–9.
2. F. P. Zamborini, M. C. Leopold, J. F. Hicks, P. J. Kulesza, M. A. Malik, and R. W. Murray, *J. Am. Chem. Soc.*, 2002, **124**, 8958–64.
3. E. S. Toberer, L. L. Baranowski, and C. Dames, *Annu. Rev. Mater. Res.*, 2012, **42**, 179–209.
4. M. D. Losego and D. G. Cahill, *Nat. Mater.*, 2013, **12**, 382–4.
5. W.-L. Ong, S. M. Rupich, D. V Talapin, A. J. H. McGaughey, and J. A. Malen, *Nat. Mater.*, 2013, **12**, 410–5.
6. B. Pelaz, S. Jaber, D. J. de Aberasturi, V. Wulf, T. Aida, J. M. de la Fuente, J. Feldmann, H. E. Gaub, L. Josephson, C. R. Kagan, N. A. Kotov, L. M. Liz-Marzán, H. Mattoussi, P. Mulvaney, C. B. Murray, A. L. Rogach, P. S. Weiss, I. Willner, and W. J. Parak, *ACS Nano*, 2012, **6**, 8468–83.
7. M. Yuan, D. Zhitomirsky, V. Adinolfi, O. Voznyy, K. W. Kemp, Z. Ning, X. Lan, J. Xu, J. Y. Kim, H. Dong, and E. H. Sargent, *Adv. Mater.*, 2013, **25**, 5586–92.
8. Y. Joseph, I. Besnard, M. Rosenberger, B. Guse, N. Heinz-Georg, J. M. Wessels, U. Wild, A. Knop-Gericke, D. Su, R. Schlogl, A. Yasuda, and T. Vossmeyer, *J. Phys. Chem. B*, 2003, **107**, 7406–7413.
9. P. Joanis, M. Tie, and A.-A. Dhirani, *Langmuir*, 2013, **29**, 1264–72.
10. B. L. V Prasad, C. M. Sorensen, and K. J. Klabunde, *Chem. Soc. Rev.*, 2008, **37**, 1871–83.
11. K. Müller, G. Wei, B. Raguse, and J. Myers, *Phys. Rev. B*, 2003, **68**, 155407.
12. Z. Peng, Y. Sun, X. Zhou, Y. Wang, D. Han, and Z. Niu, 2013, **8**, 6544–6552.
13. J. M. Beebe, V. B. Engelkes, L. L. Miller, and C. D. Frisbie, *J. Am. Chem. Soc.*, 2002, **124**, 11268–9.
14. L. Luo, S. H. Choi, and C. D. Frisbie, *Chem. Mater.*, 2011, **23**, 631–645.
15. N. D. Lang and C. R. Kagan, *Nano Lett.*, 2006, **6**, 2955–8.
16. C. Shen, C. Hui, T. Yang, C. Xiao, J. Tian, L. Bao, S. Chen, H. Ding, and H. Gao, *Chem. Mater.*, 2008, **20**, 6939–6944.
17. A. T. Fafarman, W. Koh, B. T. Diroll, D. K. Kim, D.-K. Ko, S. J. Oh, X. Ye, V. Doan-Nguyen, M. R. Crump, D. C. Reifsnyder, C. B. Murray, and C. R. Kagan, *J. Am. Chem. Soc.*, 2011, **133**, 15753–61.
18. A. Caragheorgheopol and V. Chechik, *Phys. Chem. Chem. Phys.*, 2008, **10**, 5029–41.
19. G. R. Wang, L. Wang, Q. Rendeng, J. Wang, J. Luo, and C.-J. Zhong, *J. Mater. Chem.*, 2007, **17**, 457.
20. J. A. Malen, S. K. Yee, A. Majumdar, and R. A. Segalman, *Chem. Phys. Lett.*, 2010, **491**, 109–122.
21. N. Fishelson, I. Shkrob, O. Lev, J. Gun, and A. Modestov, *Langmuir*, 2001, 403–412.
22. D. J. Wold, R. Haag, M. A. Rampi, and C. D. Frisbie, *J. Phys. Chem. B*, 2002, **106**, 10–13.
23. G. Peng, M. Strange, K. S. Thygesen, and M. Mavrikakis, *J. Phys. Chem. C*, 2009, **113**, 20967–20973.

24. J. A. Malen, P. Doak, K. Baheti, T. D. Tilley, R. A. Segalman, and A. Majumdar, *Nano Lett.*, 2009, **9**, 1164–9.
25. P. Anderson, *Phys. Rev. Lett.*, 1975, 953–955.
26. Y. X. Zhou, F. Jiang, H. Chen, R. Note, H. Mizuseki, and Y. Kawazoe, *J. Chem. Phys.*, 2008, **128**, 044704.
27. J. R. Widawsky, P. Darancet, J. B. Neaton, and L. Venkataraman, *Nano Lett.*, 2012, **12**, 354–8.
28. K.-H. Müller, *J. Chem. Phys.*, 2008, **129**, 044708.